Three-lobed Shape Bifurcation of Rotating Liquid Drops

K. Ohsaka and E. H. Trinh*

Jet Propulsion Laboratory, California Institute of Technology, Pasadena, California 91109

Abstract

The evolution of axisymmetric equilibrium shapes of a rotating liquid drop can be extended beyond the 2-lobed shape bifurcation point if the rotating drop is driven in the n=2 axisymmetric shape oscillation (perturbation), where n is the mode of oscillation. A reason for the extended stability of the perturbed rotating drop is that the inertia of the driven axisymmetric shape oscillation suppresses growth of a natural non-axisymmetric shape fluctuation which leads to the 2-lobed shape bifurcation. The axisymmetric shape of the drop eventually bifurcates into either a 2- or 3-lobed shape at a higher bifurcation point which is asserted to be the 3-lobed shape bifurcation point.

PACS numbers: 47.55.Dz

The shape evolution of a rotating liquid drop subjected to an increasing angular velocity (or momentum) has been a subject of long-standing interest since it is related to various phenomena ranging from atomic nuclear fission to planetary rotation [1]. When a spherical liquid drop, held together only by surface tension, is rotated about a vertical axis, its shape evolves into a family of axisymmetric oblate spherical shapes. The gyrostatic equilibrium shape of the drop is determined by the force balance between the capillary force created by the surface tension of the curved drop surface and the centrifugal force. With increasing angular velocity, the drop is flattened more and more until a neutral stability point is reached (a bifurcation point). By employing a method of moments, Chandrasekhar [2] showed that a family of 2-lobed equilibrium shapes were most likely evolved from the axisymmetric shape family at this bifurcation point which was denoted Ω_2 ($\simeq$ 0.559) in the normalized angular velocity scale. Brown and Scriven [3] extended Chandrasekhar's result by studying the three dimensional equilibrium shapes and stability of rotating drops using a computer-aided analytical technique. Brown-Scriven's results are summarized as follows: The neutral stability points of the axisymmetric shapes for bifurcating into the 3- and 4-lobed shapes exist at higher angular velocities. The bifurcation points are basically the same whether the drop is rotating at constant velocity or constant momentum. All axisymmetric shapes rotating above Ω_2 are unstable to a 2-lobed shape perturbation. The 2-lobed shape family is only stable when the drop is rotating at constant angular momentum. The 3-lobed shape family bifurcates at Ω_3 ($\simeq$ 0.707), but is unstable to a 2-lobed shape perturbation. The 4-lobed shape family bifurcates at Ω_4 ($\simeq$ 0.753), but is unstable to both the 2- and 3-lobed shape perturbations whether the drop is rotating at constant angular velocity or constant angular momentum.

Experimental investigations of rotating drops can be traced back to Plateau's work [4] in which a liquid drop is immersed in a liquid of similar density and is driven by a rotating shaft. Plateau observed that the drop evolved through a sequence of shapes, axisymmetric, ellipsoidal and 2-lobed shapes, and eventually broke away from the shaft. Plateau's

experimental setting roughly corresponds to the Brown-Scriven analysis with constant angular velocity. Subsequently, several experimental investigations were performed to test theoretical predictions [5-8]. Wang et al. [5,8] performed the experiments onboard the Space Shuttle in which a microgravity environment was realized. Under microgravity conditions, the drop deformation due to the Earth gravity is minimized to a negligible level; thus, the experiment can be performed in the conditions which are assumed in the theory. Wang et al's experimental setting consists of acoustic levitation of a drop in air and exerting an acoustic torque on it, which corresponds to the Brown-Scriven analysis with constant angular momentum. Wang et al. confirmed that the experimental Ω_2 for spherical drops free from deformation closely agreed with the theoretical prediction. In addition, they also showed families of shape evolution diagram for initially flattened drops, with the spherical drop as the limiting case [8].

According to the Brown-Scriven analysis, the axisymmetric shapes beyond Ω_2 are unstable to small fluctuations in shape, which grow in time; thus, it seems impossible to experimentally observe the existence of Ω_3 and Ω_4. On the contrary, one of the present authors (E. Trinh) has observed the 3-lobed shape bifurcation using an apparatus similar to the Plateau apparatus. As a proof of his observation, a photo of the 3-lobed drop is shown in Figure 1 without describing details of the experimental procedure. This observation was made possible by rapidly increasing the angular velocity of the shaft passing through the 2-lobed bifurcation point. The differential flow inside of the drop prevented the 2-lobed shape to develop before the angular velocity reached the 3-lobed bifurcation point. As is seen in the figure, the drop is not isolated but supported by the rotating shaft and the disc and its lobs are bent because of drag created by the host fluid. Applications of the same technique to an isolated drop levitated in gas environments have not been successful. As an alternative, we have come up with an idea to apply a perturbation which is favorable for axisymmetric shapes and allows us to maintain the axisymmetric shapes beyond Ω_2. In this letter, we report a technique which can suppress the 2-lobed shape bifurcation and

maintain the axisymmetric shapes until the drop reaches a higher bifurcation point, and present evidence of 3-lobed shapes evolving at the higher bifurcation point.

Figure 2 shows the experimental apparatus originally assembled for a previous study [7] and later modified for the present investigation. The ultrasonic driver is operated at approximately 18 kHz and is used to generate a vertical standing wave between the driver head and the reflector for levitating a drop. Two broadband audio drivers (the second one is not shown) are placed at the bottom corners of the chamber and are facing each other at a 90° angle. These drivers are operated at approximately 1.4 kHz and are used to generate lateral standing waves in the acoustic chamber. A torque is exerted on the drop by adjusting the relative phase of the lateral standing waves [9]. Two cameras are used to record the images of the levitated drop. Camera 1 is used to record the side view of the drop which is generally deformed into an oblate spheroid due to the acoustic pressure. The images are used to determine the volume and the aspect ratio a/b, where a and b are the equatorial and polar radii of the drop, respectively. Camera 2 is set to look down the drop through the hole made on the reflector and is capable of capturing the images up to 2000 frames per second. Small air bubbles deliberately implanted in the drop as markers are used to determine the rotation rate by reviewing the recorded images frame by frame. The angular velocity and the corresponding radius are paired to construct the shape evolution diagram. No active temperature controls are employed, but the temperature inside of the chamber remains between 28 and 29 °C throughout the measurement.

The strategy for suppressing the 2-lobed shape bifurcation is to apply a small axisymmetric n=2 shape oscillation to the rotating drop, where n is the mode of the shape oscillation (perturbation). The idea of the perturbed rotating drop is based on an expectation that the inertia of a driven n=2 axisymmetric shape oscillation prevents growth of a natural non-axisymmetric shape fluctuation that leads to the 2-lobed bifurcation. In order to induce the n=2 shape oscillation on the drop, we modulate the acoustic pressure for levitating the drop at an appropriate frequency [10,11]. A preliminary experiment with

pure water drops was not successful probably due to high surface tension and low viscosity of water; therefore, we prepared a solution which was a mixture of water (150 cc), PhotoFlo (0.2 cc) and glycerin. PhotoFlo was added to lower the surface tension value to 26 mN/m. The addition of glycerin improved the stability of the flattened drops. The drops of the solution with $1.0 \leq R_0 \leq 1.3$ mm, where, R_0 is the radius of the equivalent spherical drop, are mainly used in the present investigation. However, it is observed that only the drops with the narrower radius range, $1.2 < R_0 < 1.3$ mm are more likely to maintain the axisymmetric shapes beyond Ω_2. A reason for this observation is the modulation frequency which is set at around 80 Hz.

The results of the present investigation are summarized in Figure 3 as a plot of the normalized angular velocity, ω/ω_0, vs. the normalized radius, R_{max}/R_0, where ω is the angular velocity, $\omega_0 = 2\pi(8\sigma/\rho R_0^3)^{1/2}$ is the n=2 shape oscillation frequency of the drop with σ being the surface tension and ρ the density, and R_{max} is the maximum length of the drop in the equatorial plane. The open circles represent the data obtained by two drops (R_0 = 1.0 and 1.3 mm) which are rotated without the axisymmetric n=2 shape perturbation and used to determine the 2-lobed shape bifurcation point. The measurements were performed during both increasing and decreasing angular momentum conditions. The scattering of the data is partially due to the difference in the aspect ratio of the drops at rest. When the drop was rotated with the axisymmetric n = 2 shape perturbation, in some cases, it started evolving into the 2-lobed shape at Ω_2, but the evolution was prematurely terminated and the axisymmetric shape was restored and maintained until it reached a higher bifurcation point, Ω_h. In other cases, bifurcation at Ω_2 was not notable and the drop seemed to maintain the axisymmetric shape until it reached at Ω_h. The open triangles represent Ω_h of 6 drops which are evolved into either the 2- or 3-lobed shapes. No drops bifurcated at angular velocities between Ω_2 and Ω_h. When the drop evolved into the 2-lobed shape at Ω_h, it rapidly expanded due to excess angular momentum. The solid circles represent the 2-lobed shape drop after the instantaneous expansion of the shape bifurcated at Ω_h. The 3-lobed

shapes observed in this study were not gyrostatic equilibrium shapes, but periodically changed as the drop oscillated. The solid triangles represent the evolution of the 3-lobed shapes of the drops bifurcated at Ω_h. The solid lines are a partial reproduction of Brown-Scriven's shape evolution diagram for rotating drops at constant angular momentum. As seen in the figure, the experimental data are poorly represented by the theoretical curves. The main reason for this disagreement is due to the drop flattening which is unavoidable in ground-based experiments.

Figure 4 shows a sequence of the rotating drop with the 3-lobed shapes. As is seen, these 3-lobed shapes are not gyrostatic equilibrium shapes but are constantly changing as the drop rotates. The sequence approximately represents one cycle of the oscillation and one third of the rotation. The rotation rate and the oscillation rate are approximately 26 cycle/sec and 80 Hz, respectively. The amplitude of the oscillation is proportional to the modulation amplitude and the drop shapes in the figure are produced by a relatively high amplitude modulation. In general, the 3-lobed shapes could be maintained for tens of seconds but they subsequently evolved into the 2-lobed shapes. When the modulation was turned off, the 3-lobed shape immediately evolved into a 2-lobed shape. When the acoustic torque was gradually reduced, in some occasions, we observed that the 2-lobed shapes evolved into the 3-lobed shapes and then the axisymmetric shapes. We tried to form the 4-lobed shapes by extending the axisymmetric shape beyond Ω_h, but have not succeeded yet.

We have shown that a rotating liquid drop can maintain the axisymmetric shapes beyond Ω_2 if the drop is perturbed by the axisymmetric n=2 shape oscillation because the driven perturbation prevents the 2-lobed shape bifurcation. However, the drop eventually reaches Ω_h, and bifurcates into either the 2-lobed shape or the 3-lobed shape. Although the shape evolution diagram of initially flattened drops is different from that of spherical drops, we can reasonably assert that Ω_h corresponds to Ω_3 of spherical drops because its relative position with respect to Ω_2 is comparable to that of the theoretical curves. Lee et al. [12] have analyzed the 2-lobed bifurcation point of the initially flattened drops and have shown

that Ω_2 shifts toward lower angular velocity as the initial aspect ratio of the drop increases. Although, the analysis does not extend to the 3-lobed bifurcation point, it is plausible to assume that Ω_3 exhibits a similar shift. Furthermore, the formation of the 3-lobed shapes at Ω_h strongly supports the present assertion. We believe that the 3-lobed shape bifurcation initiates the 3-lobed shape oscillation. The direct comparison with the Brown-Scriven prediction is possible if the experiment is performed in a microgravity environment using an apparatus which is similar to the one used by Wang et al.[8]. More rigorous interpretation of the present results requires theoretical analysis of the bifurcation of the initially flattened drops driven in a shape oscillation (forced perturbation). We speculate that the present result is an example of more general bifurcation conditions which determine the mode of perturbation that selectively promotes or suppresses particular bifurcations .

The research described in this letter was carried out at the Jet Propulsion Laboratory, California Institute of Technology, under contract with the National Aeronautics and Space Administration.

References

* Currently at the NASA Headquarters, Washington D.C.

[1] N. Bohr and J. A. Wheeler, Phys. Rev. **56**, 426 (1939); S. Cohen, R. Plasil and W. J. Swiatecki, Annls Phys. **82**, 557 (1974); W. J. Swiatecki, Proc. Intl. Colloqui. on Drops and Bubbles (ed. D. J. Collins, M. S. Plesset and M. M. Saffren), JPL Pasadena (1974).

[2] S. Chandrashekar, Proc. R. Soc. London **A286**, 1 (1965).

[3] R. A. Brown and L. E. Scriven, Proc. R. Soc. London **A371**, 331 (1980).

[4] J. A. F. Plateau, Ann. Rep. to the Board of Regents of the Smithsonian Institution, pp. 270-285, Washington D.C. (1863).

[5] T. G. Wang, E. H. Trinh, A. P. Croonquist and D. D. Elleman, Phys. Rev. Lett. **56**, 452 (1986).

[6] W. K. Rhim, E. H. Trinh, S. Chung and D. D. Elleman, MRS Symposium Proc. **87**, 329 (1987).

[7] A. Biswas, E. W. Leung and E. H. Trinh, J. Acoust. Soc. Am. **69**, 1634 (1991).

[8] T. G. Wang, A. V. Anilkumar, C. P. Lee and K. C. Lin, J. Fluid Mech. **276**, 389 (1994).

[9] F. H. Busse and T. G. Wang, J. Acoust. Soc. Am. **69**, 1635 (1981).

[10] P. L. Marston and R. E. Apfel, J. Colloid Interface Sci. **68**, 280 (1979).

[11] E. H. Trinh, D. B. Thiessen and R. G. Holt, J. Fluid Mech. **364**, 253 (1998).

[12] C. P. Lee, A. V. Anilkumar, A. B. Hmelo and T. G. Wang, J. Fluid Mech. **354**, 43 (1998).

Captions

Figure 1. An example of the drop rotating in the 3-lobed shape.

Figure 2. Schematic diagram of experimental apparatus showing the key parts.

Figure 3. Summary of the results plotted in the normalized angular velocity vs. normalized radius coordinates along with the theoretical prediction.

Figure 4. A sequence of a rotating drop evolved at the 3-lobed shape bifurcation point.

TOP
↑

Fig. 1

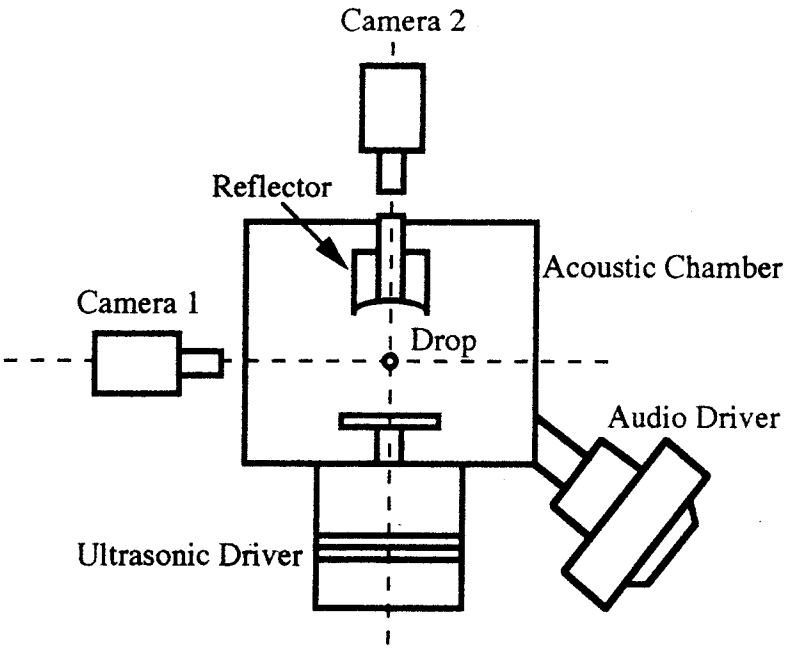
Camera 2
Reflector
Acoustic Chamber
Camera 1
Drop
Audio Driver
Ultrasonic Driver

Fig. 2

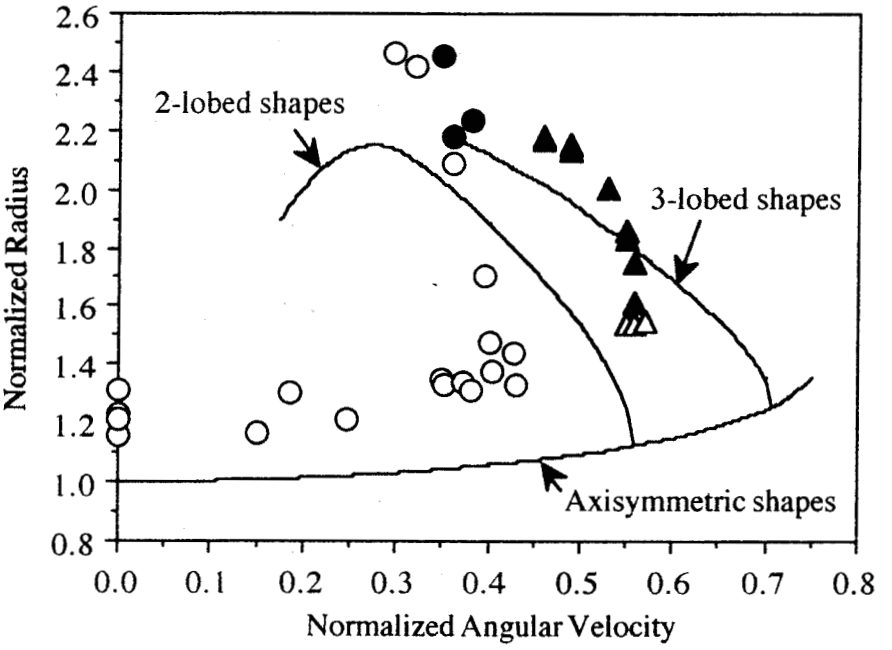
2-lobed shapes
3-lobed shapes
Axisymmetric shapes
Normalized Radius
Normalized Angular Velocity
2.6
2.4
2.2
2.0
1.8
1.6
1.4
1.2
1.0
0.8
0.0
0.1
0.2
0.3
0.4
0.5
0.6
0.7
0.8

Fig.3

Fig. 4